

Chemistry in disks

I - Deep search for N_2H^+ in the protoplanetary disks around LkCa 15, MWC 480, and DM Tau. \star

Anne Dutrey¹, Thomas Henning², Stéphane Guilloteau¹, Dmitry Semenov², Vincent Piétu³, Katharina Schreyer⁴,
Aurore Bacmann¹, Ralf Launhardt², Jérôme Pety³, Frederic Gueth³

¹ L3AB, Observatoire de Bordeaux, 2 rue de l'Observatoire, BP 89, F-33270 Floirac, France

² Max-Planck-Institut für Astronomie, Königstuhl 17, D-69117 Heidelberg, Germany

³ IRAM, 300 rue de la piscine, F-38406 Saint Martin d'Hères, France

⁴ Astrophysikalisches Institut und Universitäts-Sternwarte, Schillergässchen 2-3, D-07745 Jena, Germany

Apr 7, 2006 / Nov 21, 2006

ABSTRACT

Aims. To constrain the ionization fraction in protoplanetary disks, we present new high-sensitivity interferometric observations of N_2H^+ in three disks surrounding DM Tau, LkCa 15, and MWC 480.

Methods. We used the IRAM PdBI array to observe the N_2H^+ $J=1-0$ line and applied a χ^2 -minimization technique to estimate corresponding column densities. These values are compared, together with HCO^+ column densities, to results of a steady-state disk model with a vertical temperature gradient coupled to gas-grain chemistry.

Results. We report two N_2H^+ detections for LkCa 15 and DM Tau at the 5σ level and an upper limit for MWC 480. The column density derived from the data for LkCa 15 is much lower than previously reported. The $[\text{N}_2\text{H}^+/\text{HCO}^+]$ ratio is on the order of 0.02–0.03. So far, HCO^+ remains the most abundant observed molecular ion in disks.

Conclusions. All the observed values generally agree with the modelled column densities of disks at an evolutionary stage of a few million years (within the uncertainty limits), but the radial distribution of the molecules is not reproduced well. The low inferred concentration of N_2H^+ in three disks around low-mass and intermediate-mass young stars implies that this ion is not a sensitive tracer of the overall disk ionization fraction.

Key words. Stars: circumstellar matter – planetary systems: protoplanetary disks – individual: LkCa 15, MWC 480, DM Tau – Stellar Properties Radio-lines: stars

1. Introduction

A comprehensive understanding of the chemical composition and evolution of protoplanetary disks is a necessary prerequisite to set up the physical and chemical conditions in which planet formation should occur. Apart from CO and its isotopologues, and occasionally HCO^+ , the molecular content of protoplanetary disks remains poorly known. Dutrey et al. (1997) first reported the discovery of a number of simple molecules (HCN, CN, C_2H , H_2CO , and CS) in the circumstellar disk of DM Tau and the circumbinary disk of GG Tau, using the

IRAM 30-m telescope, while Kastner et al. (1997) observed HCN, HCO^+ , and CO in TW Hydra. Single-dish observations of molecular lines have also been reported for LkCa 15 (van Zadelhoff et al. 2001; Thi et al. 2004) and for AB Auriga by Semenov et al. (2005).

More recently, millimeter arrays have started to search for molecular lines in the protoplanetary disks of LkCa 15 (Aikawa et al. 2003; Qi et al. 2003) and TW Hydra (Qi et al. 2004). However, high-angular resolution observations are extremely scarce and often noisy. Moreover, the simultaneous detection of the continuum emission from the dust disk can bias the determination of the line intensity if not properly taken into account.

Since molecular line data are limited in sensitivity and in spatial resolution, little is known about the spatial distribution of molecules and their abundances in disks. As a consequence, comparison with existing chemical models are hampered and often based on global data (e.g. the total number of molecules

Send offprint requests to: Anne Dutrey, e-mail: anne.dutrey@obs.u-bordeaux1.fr

\star Based on observations carried out with the IRAM Plateau de Bure Interferometer. IRAM is supported by INSU/CNRS (France), MPG (Germany) and IGN (Spain). Research partially supported by PCMI, the French national program for the Physics and Chemistry of the Interstellar Medium.

or, at best, integrated line profiles). With these integrated quantities, it is difficult to test the validity of sophisticated models, which include thermal structure and even time dependency.

Using the IRAM PdBI array, we started in 2004 the CID project ("Chemistry In Disks"), a molecular survey of well-known disks such as those surrounding LkCa 15, MWC 480, and DM Tau. Our main goal was to map sufficiently strong molecular lines already detected in several disks with enough sensitivity to derive molecular abundance variations versus radius. Among the molecules we searched for, molecular ions such as HCO^+ or N_2H^+ are of great interest because they are potential tracers of the ionization structure of the disks. Note that the latter molecular ion is usually used as a high-density tracer in dense molecular cloud cores as it is supposed to barely freeze out onto dust grains even at low temperatures (e.g. Crapsi et al. 2005).

In this first paper of a series we report the observations of N_2H^+ in three objects: DM Tau, LkCa 15, and MWC 480. Using the χ^2 -minimization technique in the UV plane as described in Guilloteau & Dutrey (1998; see also Piétu et al. 2007, for details), we estimate the column density of N_2H^+ in the outer parts of these disks and the corresponding uncertainties. We compare these observed values with the N_2H^+ column densities computed with realistic 2-D steady-state disk models and a gas-grain chemistry with surface reactions. We also briefly discuss the observed properties of HCO^+ in these disks (using results from Piétu et al. 2007) and deduce an estimate of the ionization fraction.

In Sect. 2, we describe the observations and the sample of stars. The results are given in Sect. 3. Sect. 4 is dedicated to the corresponding chemical modelling. We discuss their implications in Sect. 5, followed by conclusions.

2. Sample of stars and observations

2.1. Sample of stars

Table 1 gives the coordinates and the physical properties of the observed stars. Our stars have spectral types ranging from M1 to A4. We chose these objects because they have large dust and molecular disks. Moreover, these stars are located in a hole or at an edge of their parent molecular cloud, in a region devoid of CO emission.

2.2. Observations

Observations of N_2H^+ were carried out in November 2004 and in April and September 2005. The observing time was shared in each track between LkCa 15, MWC 480, and DM Tau. The D configuration was used with 6 antennas. The sources were observed in time-sharing mode during 3 transits, leading to a total on source integration time of about 6 hours for each object. At 3 mm, the tuning was single-side-band (SSB). The backend was a correlator with three bands of 20 MHz (spectral resolution 0.125 km s^{-1}) centered on the N_2H^+ lines, one band of 20 MHz centered on the CS $J=5-4$ line, and 2 bands of 320 MHz for the 1.3mm and 3mm continuum, respectively. The phase and flux calibrators were 0415+379 and 0528+134.

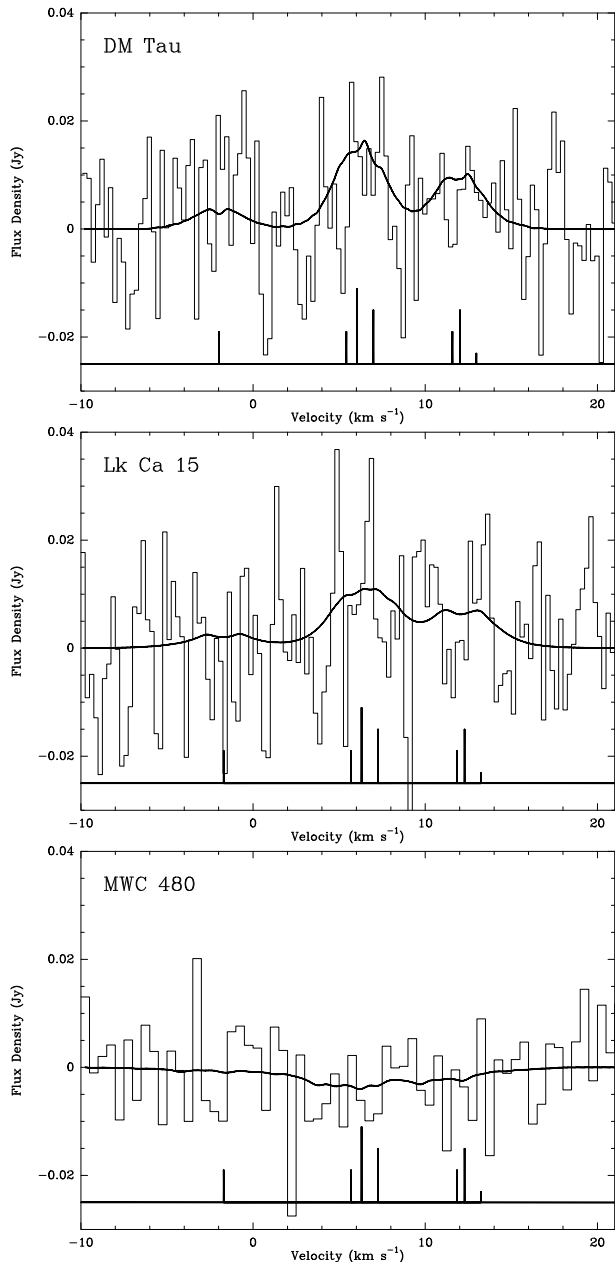


Fig. 1. Integrated spectrum of N_2H^+ $J=1 \rightarrow 0$ for DM Tau (top), LkCa 15 (middle), and MWC 480 (bottom). The thick curve represents the best model deduced from the χ^2 minimization procedure. The location and relative intensities of the hyperfine components are indicated for reference. The spectral resolution is 0.25 km s^{-1} for DM Tau and LkCa 15 and is 0.5 km s^{-1} for MWC 480. For DM Tau and LkCa 15, the lines are detected at the 5σ level, but are difficult to identify visually because of the seven hyperfine components.

Observations of HCO^+ are reported in Piétu et al. (2007). At 3 mm, the primary beam of the 15-m antennas is on the order of $56''$, or $\sim 8000 \text{ AU}$ at the Taurus distance.

For both data sets, we took great care with the relative flux calibration by using not only MWC 349 as a common reference (see the IRAM flux report, number 11) but also by always

Table 1. Sample of Stars and Stellar Properties.

Source	Right Ascension (^o , ['] , ["]), (J2000.0)	Declination (^h , ^m , ^s), (J2000.0)	Spect. Type	Effective Temp. (K)	Stellar Lum. (L _⊙)	Stellar Mass (M _⊙)	Age (Myr)	UV flux (G ₀)
LkCa 15	04:39:17.78	22:21:03.34	K5	4350	0.74	1.01 ± 0.02	3-5	2550
DM Tau	04:33:48.73	18:10:09.89	M1	3720	0.25	0.53 ± 0.03	5	410
MWC 480	04:58:46.26	29:50:36.87	A4	8460	11.5	1.83 ± 0.05	7	8500

Coordinates J 2000.0 deduced from the fit of the 1.3mm continuum map of the PdBI performed in Piétu et al. (2007). Col.3,4, 5, and 7 are the spectral type, effective temperature, the stellar luminosity and age as given in Simon et al. (2000). Masses are as given by Piétu et al. (2007). The stellar UV fluxes that are given in Col. 8 in units of the Draine (1978) interstellar UV field are taken from Bergin et al. (2004) (LkCa 15 and DM Tau) or computed from the Kurucz (1993) ATLAS9 of stellar spectra (MWC 480). They are given for a distance of 100 AU from the star.

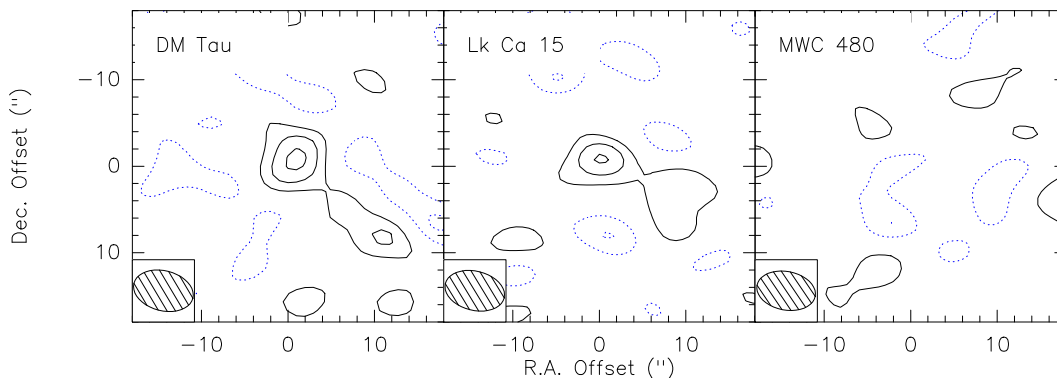


Fig. 2. Weighted intensity maps (see text for details) of N₂H⁺ J=1→0 towards DM Tau, LkCa 15, and MWC 480. The interferometric beam is 7.0'' × 4.6'', with P.A. 75° or 1000 AU × 650 AU at the Taurus distance. Contours are approximately 1.5 σ.

having our own internal reference in the observations. For this purpose we applied two methods: i) we used MWC 480 as a reference because its continuum emission is reasonably compact and bright; ii) we also checked the consistency of the flux calibration using the spectral index of DM Tau, as described in Dartois et al. (2003). We cross-checked both methods and thus obtained a reliable relative flux calibration from one frequency to another. Using our method, we estimated the relative accuracy of our flux density scale to be significantly better than 10% at 3 mm.

3. Results

Integrated spectra (over a 6'' × 6'' region) are displayed in Fig. 1, superimposed with the best-fit disk model, as derived from the disk modelling described below.

The N₂H⁺ J=1→0 emission is very weak, and determination of the integrated area is complicated by the hyperfine structure. Furthermore, due to the Keplerian velocity gradient, some components overlap in velocity. Half of the signal is in the satellite components: computing the integrated line flux would require us to include these low S/N data using twice more bandwidth than for the main group. This would degrade the overall S/N ratio. To better illustrate the detection, we instead applied a filter in which each channel is weighted by the expected line intensity (obtained from the best fit), and the sum over channels was normalized by the sum of weights, a classical optimal fil-

tering. This method confirms the detection but does not provide a quantitative estimate, which is given by the minimization (see below). The resulting weighted intensity maps are displayed in Fig. 2. Weak but significant detections are visible at the position of DM Tau and LkCa 15, but no signal is detected towards MWC 480.

The column density of N₂H⁺ is not a directly observable quantity, but it must be deduced from the map intensities, taking the line formation mechanism into account. In the analysis of disk line data the surface density is often assumed to be a power law, and then the power law index is fixed during the analysis. In this paper we follow a different approach by applying a minimization technique that results both in the N₂H⁺ column density and the power law index.

Since the analysis of the N₂H⁺ J=1→0 line is complicated by its hyperfine structure, we decided to estimate the N₂H⁺ column density by directly comparing the interferometric data to molecular disk models. Following Guilloteau & Dutrey (1998), the data were analyzed inside the *UV* plane. For each source, we fit a passive Keplerian disk model that assumes power-law radial dependencies for the molecular rotation temperature ($T_r(r) = T_{100} \times (\frac{r}{100\text{AU}})^{-q}$) and the surface density ($N_{\text{N}_2\text{H}^+}(r) = N_{100} \times (\frac{r}{100\text{AU}})^{-p}$). We assume hydrostatic equilibrium with a scale height derived from the CO measurements (see Piétu et al. 2007), and a fixed local line-width Δv . The model also takes into account the stellar mass (Table 1) and disk inclination (Table 2). The disk parameters were taken as

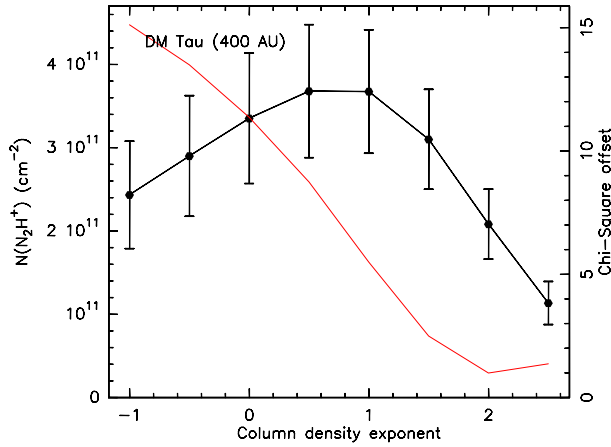


Fig. 3. Surface density of N_2H^+ at 400 AU (with error bars) versus radial exponent for DM Tau, the error bars are for ± 1 formal σ . The units are specified on the left Y axis. The light grey curve is the χ^2 (with an offset), with units on the right Y axis.

constant during the χ^2 minimization process. Only the surface-density law parameters (N_{100} and p) of N_2H^+ were varied during the minimization process. For thermalized lines such as CO $J=1-0$ and $J=2-1$ or $HCO^+ J=1-0$, the rotation temperature is a direct estimate of the gas kinetic temperature. In our case, we take the rotation temperature law from HCO^+ data (see Table 3 and Piétu et al. 2007, for details). Such a low temperature implies that the $HCO^+ J=1-0$ emission is coming from the mid-plane. Given the expected temperature range that is measured in these disks (see Tables 2-3), the chosen values have little influence on the derived column density.

The results of the fits are summarized in Table 3 and presented in Fig. 3 for DM Tau and in Fig. 4 for LkCa 15, respectively. We have chosen to show the results at 400 AU for DM Tau (300 AU for LkCa15) because it is the relevant scale for the IRAM data in terms of sensitivity and resolution. These figures indicate that we detected N_2H^+ at the $4-5\sigma$ level in both sources, with a best-fit exponent of $2-2.5$. For MWC 480, the formal best fit leads to negative column densities, at the 1σ level: we thus only mention a 3σ upper limit for this source.

The 5σ detection in LkCa 15 corresponds to a column density that is apparently about a factor ~ 100 below the column density deduced from OVRO data by Qi et al. (2003), who report an observed value of $1.7 \cdot 10^{13} \text{ cm}^{-2}$. The difference can be traced down to several factors. Qi et al. (2003) indicate a total line flux of 0.3 Jy km/s (from their Table 1), while our best fit line flux is 0.15 Jy km/s . Furthermore, Qi et al. (2003) use a constant temperature of 30 K, and give the beam-averaged column density ($p = 0$), which corresponds to a source radius of $\sim 280 \text{ AU}$. Under the same conditions, we derive a column density of $4.5 \pm 0.9 \cdot 10^{12} \text{ cm}^{-2}$. Assuming that the Qi et al. (2003) flux corresponds to the main group of hyperfine components resolves the discrepancy and shows we have detected 4 times less N_2H^+ molecules than claimed by Qi et al. (2003) if we take the same conditions for the analysis. Part of the difference may be due to the treatment of the continuum: when comput-

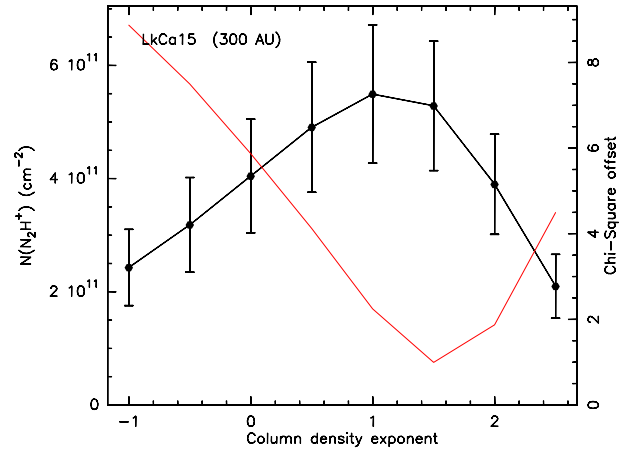


Fig. 4. Surface density of N_2H^+ at 300 AU (with error bars) versus radial exponent p for LkCa 15, the errors bars are for ± 1 formal σ . The units are specified on the left Y axis. The light grey curve is the χ^2 (with an offset), with units on the right Y axis.

Table 2. Disk Parameters

Source	i ($^\circ$)	R_{out} (AU)	T_{100} (K)	Acc.Rate ($M_\odot \text{ yr}^{-1}$)	Disk Mass (M_\odot)
DM Tau	-32	800	15, $q \sim 0.5$	$2 \cdot 10^{-9}$	0.05
LkCa 15	52	680	15, $q \sim 0.5$	10^{-8}	0.03
MWC 480	38	695 ^a	30, $q \sim 0.5$	10^{-8}	0.03

^a This value is taken from Thi et al. (2004).

Col.2 Inclinations are taken from Simon et al. (2000). Col.3 & 4 Outer radius and temperature are taken from the ^{13}CO interferometric analysis of Piétu et al. (2007). Note that the temperatures given here correspond to the observed (CO data) gas kinetic temperature from the cold mid-plane region and is higher in the disk intermediate layer. They are in good agreement with predictions from the model by D'Alessio and collaborators. Col.5 Accretion rates are taken as a generic value from D'Alessio et al. (1999) for MWC 480 and LkCa 15. The accretion rate for DM Tau is taken from Calvet et al. (2005). Col.6 Disk masses are from Dutrey et al. (1997) for DM Tau, Thi et al. (2004) for LkCa 15 and Mannings et al. (1997) for MWC 480.

ing the integrated emission, we subtracted the continuum while Qi et al. (2003) included it with the justification that the lines are optically thick. The assumption that the lines are optically thick clearly does not agree with intensities detected so far in disks, as $HCO^+(1-0)$ (Semenov et al. 2005; Piétu et al. 2007), $C^{18}\text{O}(1-0)$ and $^{13}\text{CO}(1-0)$ (Dartois et al. 2003), and $N_2H^+(1-0)$ are optically thin. Furthermore, even for an optically thick line the continuum should be subtracted because at a given velocity in the disk, the line emission covers only a tiny fraction of the entire continuum, which is at most dV/V_{Kepler} where dV is the local line-width and V_{Kepler} the projected rotation velocity at the disk edge (Beckwith & Sargent 1993; Guilloteau et al. 2006). Thus the integrated area of the line will be significantly overestimated if the continuum is not subtracted.

Table 3. Column densities of HCO⁺ and N₂H⁺ and abundance ratios

Source	MWC 480	LkCa 15	DM Tau
T	20	19	13
q	0.4	0.38	0.15
$N(\text{HCO}^+)$	$5.0 \pm 0.6 \cdot 10^{12}$	$8.0 \pm 0.5 \cdot 10^{12}$	$6.5 \pm 1.4 \cdot 10^{12}$
p	2.1 ± 0.5	2.5 ± 0.3	2.7 ± 1.0
R	250 AU	300 AU	400 AU
$N(\text{N}_2\text{H}^+)$	$< 3 \cdot 10^{11}$	$2.3 \pm 0.5 \cdot 10^{11}$	$1.1 \pm 0.25 \cdot 10^{11}$
p	2	2.5	2.5
R	250 AU	300 AU	400 AU
$[\text{N}_2\text{H}^+]/[\text{HCO}^+]$	< 0.06	~ 0.03	~ 0.02

T indicates the temperature (in K) at 100 AU and q the temperature exponent used to derive the column densities, taken from Piétu et al. (2007). For DM Tau and LkCa 15, in agreement with the figures, we present the results for $p = 2.5$. Column densities are in cm⁻². Values for HCO⁺ are taken from Piétu et al. (2007).

The large discrepancy between our analysis and that of Qi et al. (2003) clearly demonstrates the necessity of taking proper care of the column density distribution. When comparing molecules with different apparent extents or observed with different interferometric beams, this is fundamental in order to avoid biases due to sensitivity limitations. In our case, we found $p = 2.2 \pm 0.8$ for DM Tau and $p = 1.6 \pm 0.6$ for LkCa 15. These values are deduced from the best N₂H⁺ models and are in complete agreement with the analysis performed for the most sensitive tracer HCO⁺. Most importantly, we derive $[\text{N}_2\text{H}^+]/[\text{HCO}^+]$ under the assumption that this ratio is constant with radius. This is justified both by the above agreement between the p values and by the chemical models presented in Sect.4.

This result should serve as a warning that “observed” column densities either (i) come with assumptions for the surface density profile or (ii) are based on a fitting procedure within physical models. In our work, the terms “observed column densities” refer to values derived using the second method. The expression “modelled column densities” refers to column densities predicted by a chemical model, such as the one described in the next section.

4. Chemical modelling

Since our interferometric millimeter data are sensitivity limited, we have chosen to focus on the more prominent chemical effects. In this paper, our main goal is to reproduce the overall distribution of the observed molecular ions. Accordingly, the chemical model we use does not take into account grain growth and sedimentation. Similarly, Semenov et al. (2006) have shown that turbulent transport can modify the column densities and abundance distributions of some molecules with respect to the usual static chemical models in a number of cases. However, we do not include vertical/radial mixing here.

4.1. Model description

In order to confront the observed values with theoretical predictions, we used an updated gas-grain chemical model with surface reactions from Semenov et al. (2005). Briefly, it is based on the UMIST’95 gas-phase network (Millar et al. 1997) supplemented with surface chemistry on uniform 0.1 μm silicate grains from Hasegawa et al. (1992) and Hasegawa & Herbst (1993) and a small set of deuterium chemistry reactions (E.A. Bergin, private communication). Using measurements published during the last decade, we updated a few tens of important reaction rates in the UMIST’95 database (Vasyunin et al. 2006). Overall, our chemical network consists of 560 species made of 14 elements and about 5400 reactions.

The primary ionization sources in this model include stellar X-ray and UV radiation, interstellar UV radiation, and cosmic ray particles, and the decay of short-lived radionuclides. The adopted intensity of the un-attenuated stellar UV flux at 100 AU from the central stars are given in the last column of Table 1. We used the standard interstellar UV field of Draine (1978) and re-scaled it to match the corresponding stellar luminosities of TTauri stars according to the current limited knowledge of their UV spectra. This approach should be improved as soon as better UV data become available (see Bergin et al. 2006). Note that the UV penetration is computed using a 1-D plane-parallel approach and thus the UV intensity in a given disk location is very likely underestimated in comparison with the full 2-D radiative transfer simulations; see van Zadelhoff et al. (2003). The intensity and penetration of the stellar X-ray radiation are modelled using observational results of Glassgold et al. (2005) and Monte-Carlo simulations of Glassgold et al. (1997a,b). The corresponding un-attenuated ionization rates at 100 AU are equal to $4.5 \cdot 10^{-14} \text{ s}^{-1}$ for DM Tau, $2 \cdot 10^{-13} \text{ s}^{-1}$ for LkCa 15, and $2 \cdot 10^{-15} \text{ s}^{-1}$ for MWC 480.

Using the results of laboratory measurements by Bisschop et al. (2006, their “mixed-ice” case), we assumed that desorption energies of CO and N₂ are equal to 930 K. For all sources, we used a flared 1+1D disk model with a vertical temperature gradient similar to that of D’Alessio et al. (1999). This disk model has the $\sim 30 \text{ K}$ temperature surface at ~ 3 pressure scale heights (the CO surface where $\tau \sim 1$ for the CO J=2-1 transition) at a distance of 100 AU, in agreement with the results obtained by Dartois et al. (2003) and Piétu et al. (2007). Other disk parameters are summarized in Table 2.

With this physical and chemical model in hand and TMC1-like initial abundances, the chemical evolution is simulated over the 5 Myr (DM Tau and LkCa 15) and 7 Myr (MWC 480) evolutionary time. We repeated the modelling of the disk chemical evolution 20 times by using the same chemical network and varying its rate coefficients within their uncertainty limits, similar to Vasyunin et al. (2004) and Wakelam et al. (2005). This allows us to get first-order estimates of the intrinsic uncertainties of the theoretical abundances.

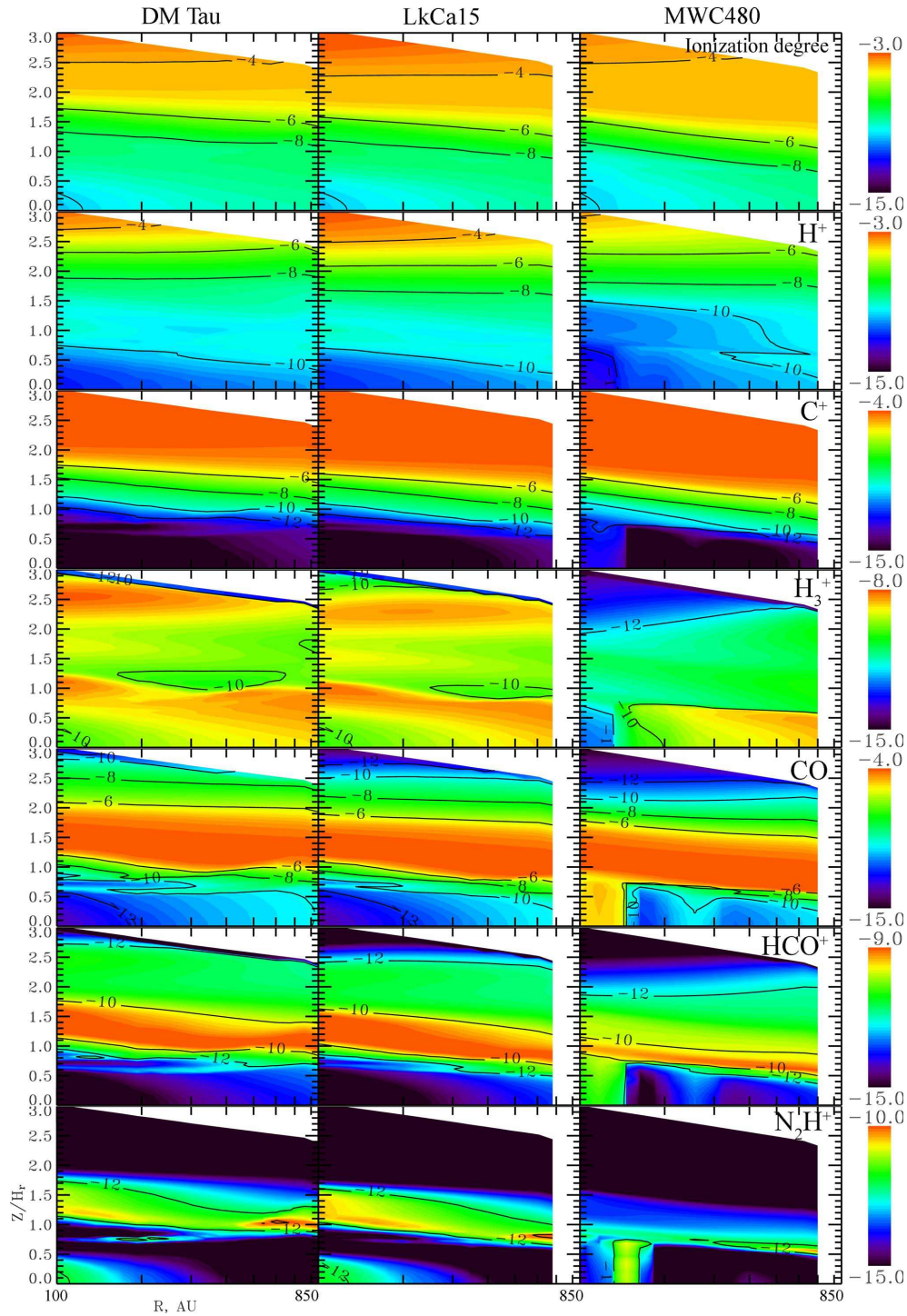


Fig. 5. From top to the bottom: model-averaged relative abundance distributions (in respect to the total number of hydrogen nuclei) of important ions: H^+ , C^+ , H_3^+ , HCO^+ , N_2H^+ , and CO in the DM Tau (left), LkCa 15 (middle), and MWC 480 (right) disks after 5 and 7 Myr of the evolution. The Y-axis is the disk vertical extent normalized by one pressure scale height (different for all three objects).

4.2. Ionization in disks and global evolution of N_2H^+ and HCO^+

In Fig. 5 we present the model-averaged disk abundances of CO , several dominant ions, and the ionization fraction after a few Myr of evolution for all three objects without mixing. The

Y-axis is expressed in units of the pressure scale height, H_r , as defined in Dartois et al. (2003).

More generally, in the upper surface layer ($\gtrsim 2$ scale heights) the dominant ion is H^+ , with an abundance up to $\sim 10^{-3}$ (with respect to the total amount of hydrogen nuclei). Somewhat lower, at $\gtrsim 1.5$ scale heights, the disk ionization de-

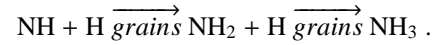
gree is determined by ionized carbon, which is also the most abundant ion in all three disks ($[C^+] \lesssim 10^{-4}$, $N(C^+) \approx N(e^-) \sim 3 \cdot 10^{16} \text{ cm}^{-2}$ around $\sim 200\text{-}500$ AU). The evolution of both ions is governed entirely by fast photo-reactions due to energetic stellar UV field and X-rays and interstellar UV radiation. In contrast, the less abundant H₃⁺ ion mostly traces the fractional ionization closer to the disk midplane, $[H_3^+] \sim [e^-] \lesssim 10^{-9}$, where the cosmic ray particles remain the only ionization source. Unfortunately, all these important ions are not easily detectable in protoplanetary disks (however, see Kamp et al. 2003; Ceccarelli & Dominik 2005).

The *observationally* most important ion in the outer disks is predicted to be HCO⁺ (typical abundance value is $\lesssim 10^{-9}$). It is located in the warm molecular layer that is partly shielded from direct ionizing radiation from the central star and the ISM, at ~ 1 pressure scale height. Note that the corresponding HCO⁺ layer is thinner and located deeper towards the midplane in the MWC 480 disk in comparison with DM Tau and LkCa 15. Such a chemical effect is caused primarily by the strong radiation field of MWC 480, which is capable of dissociating CO – the key molecule for the HCO⁺ evolution – more deeply inside the disk, as seen in the figure. The more intense stellar heating also leads to a warmer interior of the MWC 480 disk compared to the cases of DM Tau and LkCa 15, which in turn results in efficient CO desorption in the MWC 480 disk midplane at $R \lesssim 200$ AU and thus in a reservoir of abundant HCO⁺ there. Note that, in all three cases, the upper boundary of the abundant HCO⁺ layer coincides with the lower boundary of the C⁺ layer that marks the disk height where penetration of the ionizing radiation essentially stops. This happens at $\sim 1 - 1.5$ scale heights.

In contrast to HCO⁺, the next observationally important ion N₂H⁺ is concentrated in a very thin layer at the lower bottom of the intermediate layer ($\sim 0.5 - 1$ scale heights) and in the disk midplane. Unlike for other considered species, N₂H⁺ abundances are more spatially peaked toward outer disk regions. It is also interesting that the N₂H⁺ vertical layer is in general thinner in the MWC 480 disk compared to the disks around LkCa 15 and DM Tau, similar to the HCO⁺ distribution. The main reason for the chemical differentiation between these two ions is the fact that N₂H⁺ gets destroyed easily in proton transfer reactions with CO, e.g. $N_2H^+ + CO \rightarrow HCO^+ + N_2$ ($k = 8.8 \cdot 10^{-10} \text{ cm}^3 \text{ s}^{-1}$ Anicich & Huntress 1986).

Thus, N₂H⁺ is less abundant in the disk region where the CO concentration is high, that is, in the CO molecular layer above about one pressure scale height. On the other hand, it also cannot be abundant in the disk surface layer exposed to the energetic radiation from the star, which destroys all polyatomic species within $\sim 10^4$ years. Finally, it cannot reach high levels of concentration in the outer disk midplane ($R > 400$ AU in DM Tau and LkCa 15, and $R > 200$ AU in MWC 480) because the evolution of N₂H⁺ in the entire midplane region is governed by a cycle between ion-molecule reactions of N₂ with the most abundant ion, H₃⁺ ($\lesssim 10^{-9}$), and dissociative recombination of N₂H⁺ with electrons and charged grains. Consequently, at very low temperatures in the outer midplane a volatile product of the N₂H⁺ dissociation, namely NH (desorption energy is 600 K), is frozen out on grain surfaces and eventually converted to solid

NH₃ by a two-step process of surface hydrogenation:



Thus, after about 1 Myr of evolution all nitrogen is locked in solid ammonia that has an abundance of about 10^{-5} . In contrast, in the warmer disk midplane region that is located closer to the central star, NH is not totally frozen out and thus the surface formation of ammonia is not that efficient. Therefore, about 10% of all nitrogen is locked in solid N₂ ($\sim 2 \cdot 10^{-6}$), but a minor fraction of molecular nitrogen remains in the gas phase ($\sim 10^{-8}$) and reacts with H₃⁺, forming N₂H⁺.

Note that there is a thin layer devoid of N₂H⁺ at about 0.7 scale height in the disk of DM Tau at 100 AU and, to a lesser extent, LkCa 15. In contrast to the Herbig Ae star MWC 480, these two Sun-like T Tau stars are strong emitters of hard X-ray radiation (Glassgold et al. 2005). The stellar X-ray radiation cannot propagate directly through the disk midplane, but in general has larger penetration depth toward the disk interior than UV photons. Semenov et al. (2004) have shown that the attenuated X-rays can drive a peculiar chemistry leading to the production of complex (organic) species on dust grains.

5. Discussion

5.1. Observed abundances of molecular ions in disk

HCO⁺ is observed in many astrophysical media with a wide variety of physical conditions, from diffuse clouds (Liszt & Lucas 2001) up to dense cores (Caselli et al. 2002a). N₂H⁺, which can be significantly less abundant and even depleted in very dense cores (Pagani et al. 2005), appears more difficult to observe (Tafalla et al. 2004). Moreover, as described in Sect. 4.2, N₂H⁺ can be destroyed by reactions with CO to give HCO⁺ (see also, Anicich & Huntress 1986). Hence, HCO⁺ and N₂H⁺ usually do not coexist. Having abundance estimates coming from the same area is not so easy. This is, for example, illustrated by Jørgensen (2004) in L483-mm where he finds that the HCO⁺ traces the large scale outflow, while N₂H⁺ traces the quiescent material (in the core) being accelerated by the outflow (see also his Fig.13). Observations of absorption lines in diffuse clouds in front of bright quasars allow Liszt & Lucas (2001) to estimate a lower limit on the abundance ratio of $[N_2H^+]/[HCO^+] < 0.002$ (at 2σ). Aikawa et al. (2005) predict abundance ratios of $[N_2H^+]/[HCO^+]$ within the range 0.02–0.1 for physical conditions relevant for pre-stellar collapsing dense cores. These chemical models correspond to abundances of N₂H⁺ and HCO⁺, in agreement with observations of starless cores such as L1544 (Tafalla et al. 2004; Caselli et al. 2002b). To first order, we get an averaged ratio $[N_2H^+]/[HCO^+]$ on the order of $\sim 0.02 - 0.03$ (see Table 3). The abundance ratios we observe in the T Tauri disks are therefore similar to those observed and modelled in dense cores of cold molecular clouds.

5.2. Reliability of chemical model

Our non-mixing chemical model (described in Sect. 4.2) coupled to a 1+1D steady-state disk model with small sub-micron size dust grains cannot reproduce the complexity of the disk

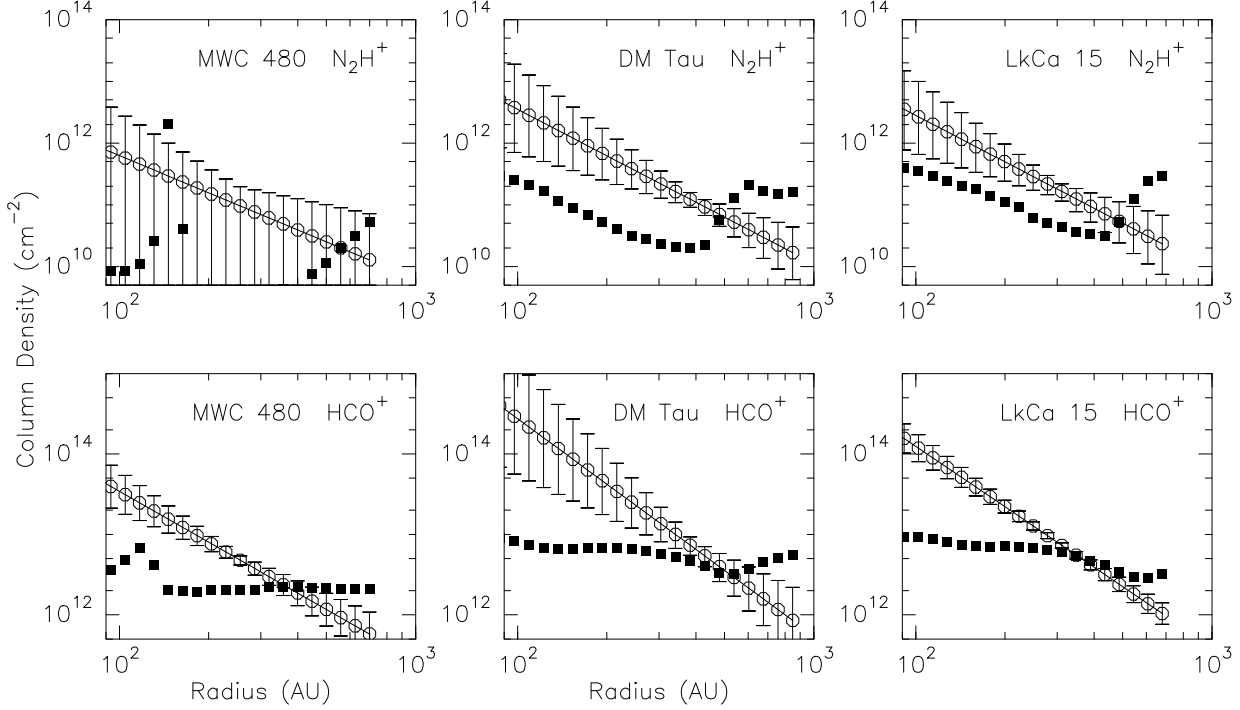


Fig. 6. Top: Expected column density of N_2H^+ versus radius (black dots), compared to the observed column densities (curve and errorbars) in MWC 480 (left), DM Tau (middle), and LkCa 15 (right). Bottom: as above but for HCO^+ . The disk age is 5 Myr for DM Tau and LkCa 15 and 7 Myr for MWC 480. The abrupt changes in predicted column densities of N_2H^+ at some radii are partly due to the limited resolution of the chemical model (see Fig. 5). For HCO^+ , the error bars include the (measured) uncertainty on the excitation temperature for DM Tau, while this excitation temperature was imposed for LkCa 15 and MWC 480

structure. Surprisingly, we are able to obtain reasonable global agreements with the observed column densities of N_2H^+ and HCO^+ around 400 AU in all three disks (see Fig. 6). But we fail to reproduce in detail the observed slopes p . The modelled N_2H^+ column density is in general too high in the outer disk ($R > 400$ AU), while the HCO^+ column density appears too low in the inner part of the disks. However, in the model as in the observations, the $[HCO^+]/[N_2H^+]$ ratio is almost constant with radius. More precisely, the value of $\sim 3 \cdot 10^{11} \text{ cm}^{-2}$ for the column density of N_2H^+ in the DM Tau disk is about 50% higher than the observed value, which is well within the error bars of a factor of 3 in the abundance due to the inaccuracy of the reaction rates in the UMIST'95 ratefile (see Vasyunin et al. 2004; Wakelam et al. 2005). The overall agreement between the modelled and observed column densities of HCO^+ in DM Tau, LkCa 15, and MWC 480 is not as good as for N_2H^+ (see Fig. 6). The observed value of about $5 \cdot 10^{12} \text{ cm}^{-2}$ that is nearly equal for the three disks is 3 times higher than predicted by the MWC 480 model and 3 times lower than obtained with the DM Tau and LkCa 15 disk models. Note that the computed HCO^+ column densities also suffer from intrinsic uncertainties caused by the reaction rate uncertainties, about a factor of 3–4.

Since the chemistry of HCO^+ is sensitive to the grain growth, the presence of large grains, as usually observed in disks with dust spectral index $\beta \approx 1 - 0.5$, may also account for the discrepancy between the results of the applied chemical models and observational data, especially for HCO^+ , but due to

the limitations of the current chemical prescription this cannot be easily checked.

5.3. Determining the disk ionization fraction

As shown in the previous section, the ionization fraction in different disk regions is dominated by distinct ions, with C^+ the most abundant one in the upper layer. Is there any possibility of estimating the degree of ionization in some disk regions or even in the entire disk?

The HCO^+ abundance gives a lower limit to the electron fraction, $[e^-] > [HCO^+]$. The H_2 column density is uncertain: taking $[^{13}CO] = 10^{-7}$ and column density values from Piétu et al. (2007) leads to $[e^-] > 2 \cdot 10^{-10}$. Following Qi et al. (2003, their Eq.6), a lower limit to $[e^-]$ can also be obtained from N_2H^+ :

$$[e^-] > [CO] \frac{k_2}{k_{rec}(HCO^+)} \frac{[N_2H^+]}{[HCO^+]} = 4.3 \cdot 10^{-4} \frac{[N_2H^+]}{[HCO^+]} \cdot [CO] \quad (1)$$

where $k_2 = 8.8 \cdot 10^{-10} \text{ cm}^3 \cdot \text{s}^{-1}$ is the reaction rate coefficient of CO with N_2H^+ ($CO + N_2H^+ \rightarrow HCO^+ + N_2$) and $k_{rec}(HCO^+) = 3 \cdot 10^{-7} (T/300)^{-0.64} \text{ cm}^3 \text{ s}^{-1}$ is the dissociative recombination rate coefficient of HCO^+ . The numerical value is for $T = 15$ K. Thus N_2H^+ can be a more sensitive tracer of the ionization fraction in disks than HCO^+ only if

$$\frac{[N_2H^+]}{[HCO^+]} > \frac{1}{4.3 \cdot 10^{-4}} \frac{[HCO^+]}{[CO]} \quad (2)$$

Table 4. Estimated ionization degrees

Source	T (K)	n_{H} cm ⁻³	ζ_X s ⁻¹	[e ⁻] (HCO ⁺)	[e ⁻] (N ₂ H ⁺)
DM Tau	15	5 10 ⁶	4 10 ⁻¹⁷	2 10 ⁻⁹	4 10 ⁻⁹
LkCa 15	15	5 10 ⁶	10 ⁻¹⁶	3 10 ⁻⁹	7 10 ⁻⁹
MWC 480	25	5 10 ⁶	1.3 10 ⁻¹⁷	2 10 ⁻⁹	3 10 ⁻⁹

Estimates of the disk ionization degree in the intermediate layer derived from chemical equilibrium approach (Eq.3), where the two values (col 5 and 6) depend on whether HCO⁺ or N₂H⁺ dominates the recombination process.

From Piétu et al. (2007), the [¹³CO]/[HCO⁺] ratio is ≈ 600 . After correction of the isotopologue column density ratio, around 20 when fractionation is accounted for (Piétu et al. 2007), we find that, if observed with a similar S/N, N₂H⁺ can be a more sensitive tracer than HCO⁺ only if [N₂H⁺]/[HCO⁺] > 0.2. With the measured abundance ratios, ~ 0.02 , HCO⁺ thus remains a better tracer of the electron abundance than N₂H⁺. Furthermore, these low abundance ratios no longer support a high value for the gas phase [N₂]/[CO] ratio.

Another simple approach, but independent of the observations, to obtain an estimate of the disk fractional ionization is to use the equation of chemical equilibrium (e.g., Gammie 1996):

$$[e^-] = \sqrt{\frac{\zeta}{k_{\text{rec}} n_{\text{H}}}}, \quad (3)$$

where ζ is the ionization rate (in s⁻¹), k_{rec} is a typical recombination rate (cm³ s⁻¹), and n_{H} is the hydrogen number density. Semenov et al. (2004) have demonstrated that the equilibrium approach is appropriate in most disk regions. For the HCO⁺ and N₂H⁺ ions, the recombination rates in our chemical network are $k_{\text{rec}} = 3 \cdot 10^{-7} (T/300)^{-0.64}$ cm³ s⁻¹ and $k_{\text{rec}} = 10^{-7} (T/300)^{-0.5}$ cm³ s⁻¹, respectively (Millar et al. 1997; Geppert et al. 2004, 2005). The steady-state values of the ionization degree in the warm molecular layers of the outer disk range are presented in Table 4. Temperatures were taken from Table 2, the density from Dartois et al. (2003), and the X-ray ionization rates from Glassgold et al. (2005). The cosmic ray rate is $1.3 \cdot 10^{-17}$ s⁻¹. The values in Table 4 are consistent with the results of the detailed chemical calculations shown in Fig. 5 (first row, one scale height and radius ~ 200 -500 AU). These values are high enough to allow magneto-rotational instability to operate in this region of the disks (see discussion in Semenov et al. 2004).

6. Summary

Using the IRAM array, we report new observations of N₂H⁺ J=1-0 in three protoplanetary disks surrounding two T Tauri stars: LkCa 15 and DM Tau and the Herbig Ae/Be star MWC 480. We analyze these data by also taking the HCO⁺ J=1-0 data from Piétu et al. (2007) into account. For the three objects, we derive from the observations the column densities and abundances and compare them to model predictions obtained using a 1+1D chemical code. Our main conclusions are the following:

- We detected N₂H⁺ (at 5 σ level) in the disks surrounding LkCa 15 and DM Tau. In the disk of LkCa 15, the column density we observed is a factor ~ 100 below previous claims.
- The N₂H⁺ column densities derived from the observations imply an [N₂H⁺]/[HCO⁺] ratio which is on the order of the ratio found in cold dense cores $\sim 0.02 - 0.03$.
- HCO⁺ remains the more abundant molecular ion in disks. A lower limit of $2 \cdot 10^{-10}$ for the ionization fraction can be obtained from the observations of HCO⁺ and ¹³CO.
- The overall column densities of N₂H⁺ and HCO⁺ and the [N₂H⁺]/[HCO⁺] ratio are approximately reproduced by the chemical models, but their radial dependencies (slope p) are not. The latter disagreement may be linked to the limits of the chemical modelling, which does not include processes like grain growth or turbulent mixing. It could also be due to an over-simplistic disk structure, since Piétu et al. (2006) have shown that the dust distribution in LkCa 15 and MWC 480 are quite different from the simple density distribution adopted here.

Acknowledgements. We acknowledge all the Plateau de Bure IRAM staff for their help during the observations. We also acknowledge the Grenoble IRAM staff for their support during the first data reduction session of the CID project in January 2006. We are thankful to Dmitry Wiebe for providing the disk physical models. The French Program of Physico-Chemistry (PCMI) is thanked for providing funding for this project. D.S. and T.H. thank the Deutsche Forschungsgemeinschaft, DFG project “Research Group Laboratory Astrophysics” (He 1935/17-2) for their support.

References

- Aikawa, Y., Herbst, E., Roberts, H., & Caselli, P. 2005, *ApJ*, 620, 330
- Aikawa, Y., Momose, M., Thi, W.-F., et al. 2003, *PASJ*, 55, 11
- Anicich, V. G. & Huntress, W. T. 1986, *ApJS*, 62, 553
- Beckwith, S. V. W. & Sargent, A. I. 1993, *ApJ*, 402, 280
- Bergin, E., Calvet, N., Sitko, M. L., et al. 2004, *ApJ*, 614, L133
- Bergin, E. A., Aikawa, Y., Blake, G. A., & van Dishoeck, E. F. 2006, in *Protostars and Planets V*, Proceedings of the Conference held October 24-28, 2005, in Hilton Waikoloa Village, Hawai’i, –+
- Bisschop, S. E., Fraser, H. J., Öberg, K. I., van Dishoeck, E. F., & Schlemmer, S. 2006, *A&A*, 449, 1297
- Calvet, N., D’Alessio, P., Watson, D. M., et al. 2005, *ApJ*, 630, L185
- Caselli, P., Walmsley, C. M., Zucconi, A., et al. 2002a, *ApJ*, 565, 331
- Caselli, P., Walmsley, C. M., Zucconi, A., et al. 2002b, *ApJ*, 565, 344
- Ceccarelli, C. & Dominik, C. 2005, *A&A*, 440, 583
- Crapsi, A., Devries, C. H., Huard, T. L., et al. 2005, *A&A*, 439, 1023
- D’Alessio, P., Calvet, N., Hartmann, L., Lizano, S., & Cantó, J. 1999, *ApJ*, 527, 893
- Dartois, E., Dutrey, A., & Guilloteau, S. 2003, *A&A*, 399, 773
- Draine, B. T. 1978, *ApJS*, 36, 595
- Dutrey, A., Guilloteau, S., & Guelin, M. 1997, *A&A*, 317, L55

- Gammie, C. F. 1996, *ApJ*, 457, 355
- Geppert, W. D., Thomas, R., Semaniak, J., et al. 2004, *ApJ*, 609, 459
- Geppert, W. D., Thomas, R. D., Ehlerding, A., et al. 2005, *Journal of Physics Conference Series*, 4, 26
- Glassgold, A. E., Feigelson, E. D., Montmerle, T., & Wolk, S. 2005, in *ASP Conf. Ser. 341: Chondrites and the Protoplanetary Disk*, 165–+
- Glassgold, A. E., Najita, J., & Igea, J. 1997a, *ApJ*, 480, 344
- Glassgold, A. E., Najita, J., & Igea, J. 1997b, *ApJ*, 485, 920
- Guilloteau, S. & Dutrey, A. 1998, *A&A*, 339, 467
- Guilloteau, S., Piétu, V., Dutrey, A., & Guélin, M. 2006, *A&A*, 448, L5
- Hasegawa, T. I. & Herbst, E. 1993, *MNRAS*, 263, 589
- Hasegawa, T. I., Herbst, E., & Leung, C. M. 1992, *ApJS*, 82, 167
- Jørgensen, J. K. 2004, *A&A*, 424, 589
- Kamp, I., van Zadelhoff, G.-J., van Dishoeck, E. F., & Stark, R. 2003, *A&A*, 397, 1129
- Kastner, J. H., Zuckerman, B., Weintraub, D. A., & Forveille, T. 1997, *Science*, 277, 67
- Kurucz, R. 1993, *ATLAS9 Stellar Atmosphere Programs and 2 km/s grid*. Kurucz CD-ROM No. 13. Cambridge, Mass.: Smithsonian Astrophysical Observatory, 1993., 13
- Liszt, H. & Lucas, R. 2001, *A&A*, 370, 576
- Mannings, V., Koerner, D. W., & Sargent, A. I. 1997, *Nature*, 388, 555
- Millar, T. J., Farquhar, P. R. A., & Willacy, K. 1997, *A&AS*, 121, 139
- Pagani, L., Pardo, J.-R., Apponi, A. J., Bacmann, A., & Cabrit, S. 2005, *A&A*, 429, 181
- Piétu, V., Dutrey, A., & Guilloteau, S. 2007, *A&A*, submitted
- Piétu, V., Dutrey, A., Guilloteau, S., Chapillon, E., & Pety, J. 2006, *A&A*, 460, L43
- Qi, C., Ho, P. T. P., Wilner, D. J., et al. 2004, *ApJ*, 616, L11
- Qi, C., Kessler, J. E., Koerner, D. W., Sargent, A. I., & Blake, G. A. 2003, *ApJ*, 597, 986
- Semenov, D., Pavlyuchenkov, Y., Schreyer, K., et al. 2005, *ApJ*, 621, 853
- Semenov, D., Wiebe, D., & Henning, T. 2004, *A&A*, 417, 93
- Semenov, D., Wiebe, D., & Henning, T. 2006, *ApJ*, 647, L57
- Simon, M., Dutrey, A., & Guilloteau, S. 2000, *ApJ*, 545, 1034
- Tafalla, M., Myers, P. C., Caselli, P., & Walmsley, C. M. 2004, *A&A*, 416, 191
- Thi, W.-F., van Zadelhoff, G.-J., & van Dishoeck, E. F. 2004, *A&A*, 425, 955
- van Zadelhoff, G.-J., Aikawa, Y., Hogerheijde, M. R., & van Dishoeck, E. F. 2003, *A&A*, 397, 789
- van Zadelhoff, G.-J., van Dishoeck, E. F., Thi, W.-F., & Blake, G. A. 2001, *A&A*, 377, 566
- Vasyunin, A. I., Semenov, D. A., Sobolev, A. M., & Henning, T. 2006, *ApJ*, in preparation
- Vasyunin, A. I., Sobolev, A. M., Wiebe, D. S., & Semenov, D. A. 2004, *Astronomy Letters*, 30, 566
- Wakelam, V., Selsis, F., Herbst, E., & Caselli, P. 2005, *A&A*, 444, 883